CHRNA5 links chandelier cells to protection against amyloid pathology in human aging and Alzheimer's Disease

Jonas Rybnicek[1], Yuxiao Chen[2], Milos Millic[2], JoAnne McLaurin[3], Philip L De Jager[4], Julie A Schneider[5], Yanling Wang[6], David A Bennett[6], **Shreejoy Tripathy*[1, 2, 7, 8], Daniel Felsky*[2, 7, 8], Evelyn K Lambe*[1, 7, 9]**

1. Department of Physiology, University of Toronto, Toronto ON, Canada

2. Krembil Centre for Neuroinformatics, Centre for Addiction and Mental Health, Toronto ON, Canada

3. Biological Sciences, Sunnybrook Research Institute, Toronto, ON M4N 3M5, Canada.

4. Center for Translational & Computational Neuroimmunology, Department of Neurology and the Taub Institute for Research on Alzheimer's Disease and the Aging Brain, Columbia University Irving Medical Center, New York NY, USA

5. Department of Pathology, Rush University, Chicago IL, USA

6. Department of Neurological Sciences, Rush University, Chicago IL, USA

7. Department of Psychiatry, University of Toronto, Toronto ON, Canada

8. Institute of Medical Science, University of Toronto, Toronto ON, Canada

9. Department of OBGYN, University of Toronto, Toronto ON, Canada

*Co-corresponding authors

Co-Corresponding Authors email addresses:

Shreejoy Tripathy: shreejoy.tripathy@camh.ca

Dan Felsky: daniel.felsky@camh.ca

Evelyn Lambe: evelyn.lambe@utoronto.ca

Number of Figures: 5

Number of Tables: 1

Word count: Abstract: 216, Introduction: 541, Discussion: 1120

Conflicts of Interest: None

Acknowledgements: This work was supported by the Canadian Institutes of Health Research (CIHR; MOP89825 and CIHR PJT-153101; EKL). DF is supported by the Krembil Foundation, Koerner Family Foundation, Canadian Institutes of Health Research, and the CAMH Discovery Fund. JM is supported by the Canadian Research Chairs program, as a Tier 1 Chair. ROSMAP is supported by P30AG10161, P30AG72975, R01AG15819, R01AG17917. U01AG46152, U01AG61356. ROSMAP resources can be requested at https://www.radc.rush.edu

Abstract

Changes in high-affinity nicotinic acetylcholine receptors are intricately connected to neuropathology in Alzheimer's Disease (AD). Protective and cognitive-enhancing roles for the nicotinic α5 subunit have been identified, but this gene has not been closely examined in the context of human aging and dementia. Therefore, we investigate the nicotinic α5 gene *CHRNA5* and the impact of relevant single nucleotide polymorphisms (SNPs) in prefrontal cortex from 922 individuals with matched genotypic and *post-mortem* RNA sequencing in the Religious Orders Study and Memory and Aging Project (ROS/MAP). We find that a genotype robustly linked to expression of *CHRNA5* (rs1979905A2) predicts significantly reduced β-amyloid load in prefrontal cortex. Yet, co-expression analysis shows a clear dissociation between expression of *CHRNA5* and other cholinergic genes, suggesting a distinct cellular expression profile for the human nicotinic α5 subunit. Consistent with this prediction, single nucleus RNA sequencing from 22 individuals reveals disproportionately-elevated *CHRNA5* expression in chandelier cells. These interneurons are enriched in amyloid-binding proteins and also play a vital role in excitatory/inhibitory (E/I) balance. Cell-type proportion analysis demonstrates that chandelier cells have increased amyloid vulnerability in individuals homozygous for the missense *CHRNA5* SNP (rs16969968A2) that impairs function/trafficking of nicotinic α5-containing receptors. These findings suggest that *CHRNA5* and its nicotinic α5 subunit exert a neuroprotective role in aging and Alzheimer's disease potentially centered on chandelier interneurons.

Keywords: Alzheimer's disease, prefrontal cortex, acetylcholine, nicotinic receptors, chandelier cells, interneurons, amyloid, attention

Introduction

The cholinergic system plays a critical role in the pathology of Alzheimer's disease (AD) (1), a neurodegenerative disease marked by the accumulation of β-amyloid peptide (β-amyloid) and neurofibrillary tangles of phosphorylated tau in the brain (2). In AD, there are well-characterized disturbances in the excitation/inhibition (E/I) balance in cerebral cortex (3,4) arising from the disruption of inhibitory signalling. The shift toward higher excitation in the cortex is associated with cognitive impairment in AD.

The cholinergic system is an important regulator of E/I balance in the prefrontal cortex (PFC) (5,6) and is central to one of the first mechanistic explanations of cognitive deficits in AD; the so-called *cholinergic hypothesis* (7). In AD, there is a decrease of cortical nicotinic acetylcholine receptor binding (8,9), and β-amyloid binding to nicotinic receptors has been postulated as a potential mediator of AD pathology (10,11) possibly via blockade of these receptors (12,13). By contrast, stimulation of nicotinic receptors has been found to improve neuronal survival in AD pathology (14), promote neurogenesis, and improve cognition (15,16). Promoting nicotinic signalling using acetylcholinesterase inhibitors is one of the mainstay AD treatments (17).

High-affinity nicotinic acetylcholine receptors are hetero-pentamer cation channels most commonly composed of α4 and β2 subunits (α4β2) (18). Deep layer PFC pyramidal cells express nicotinic receptors also containing the auxiliary α5 subunit (18,19). Nicotinic α5 subunits do not contribute to the acetylcholine binding site and cannot form functional receptors on their own (19), requiring the binding sites provided by partner subunits α4 and β2, and forming the α4β2α5 nicotinic receptor. The α5 subunit alters the kinetics of nicotinic receptors (20) and increases their permeability to calcium ions (21,22). Importantly, β-amyloid binds less readily to α4β2α5 than α4β2 nicotinic receptors (12), which raises the question of a possible protective role of the α5 subunit in AD pathology.

The nicotinic α5 subunit has previously been linked to cognitive performance, with loss or disruption of this subunit impairing performance in attentional tasks in rodents (23,24). In humans, single nucleotide polymorphisms (SNPs) affecting the expression and function/trafficking of the *CHRNA5* gene, which codes for the α5 subunit, have been linked to attentional and cognitive deficits (25,26). These SNPs are also linked to smoking (27), a major AD risk factor (28). However, the role of *CHRNA5* in aging and AD is unknown.

To address this critical gap, we built a multi-step model of the connections between SNPs affecting the expression and function of *CHRNA5*, and age-related cognitive and neuropathological phenotypes using detailed clinical and post-mortem data from the Religious Order Study and Memory and Aging Project (ROS/MAP) (29). Next, we leveraged single-nucleus RNAseq to determine the cell-type expression pattern of *CHRNA5* in the PFC. We then used a gene ontology analysis of cortical patch-seq data (30) to elucidate the functional makeup of the cell type with the highest *CHRNA5* levels in the PFC, the chandelier cells. Finally, we probed an estimated cell type proportion dataset from the PFC (31) to assess the interaction effect of *CHRNA5* SNPs and Alzheimer's disease pathology on this *CHRNA5*-enriched cell type. The results of our study suggest a novel role for *CHRNA5* in maintaining the E/I balance in the forebrain and as a potential new target for therapies aiming to promote neuronal survival in AD.

Methods

Study cohort

We accessed data from 2004 deceased individuals from the ROS/MAP cohort study (29), of whom 1732 were autopsied. Both studies enrolled individuals without known dementia. ROS enrols elderly nuns, priests, and members of clergy, whereas MAP enrols individuals from community facilities and individual homes. Both studies were approved by an Institutional Review Board of Rush University Medical Centre. Participants gave informed consent for annual clinical evaluation, completed a repository consent allowing their resources to be shared, and signed an Anatomic Gift Act for brain donation at the time of death. Most individuals assessed were female (68%). The average age at study entry was 80.5 ± 0.16 years and the average age at death was 89.2 ± 0.2 years. All data was retrieved from the Synapse AMP-AD Knowledge Portal (Synapse ID: syn2580853).

Selection of candidate single nucleotide polymorphisms (SNPs)

Nicotinic α5 subunits (encoded by *CHRNA5*) do not contribute to the acetylcholine binding site and cannot form functional receptors on their own (19). In prefrontal cortex, the nicotinic α5 subunits participate in pentameric receptors with two binding sites contributed by partner subunits: α4 (encoded by *CHRNA4*) and β2 (encoded by *CHRNB2*) (18). Together, these subunits form α4β2α5 nicotinic receptors. While the current focus is *CHRNA5*, we also probed the impact of polymorphisms relevant to its receptor partners *CHRNA4* or *CHRNB2* for perspective. The specific polymorphisms were selected based on their reported effects on expression, coding, or clinical response. (*CHRNA5*:(27,32,33); CHRNB2: (34,35),; *CHRNA4*: (36).

Genotype data preparation and imputation, quality control, generation of residuals

Details on the preparation and handling of ROS/MAP post-mortem samples have been previously published (Jager et.al 2018) and are described briefly together with the quality control approaches and generation of the residuals in **Supplement 1**.

Neuropathology and cognitive scores

The ROS/MAP neuropathology data used in our study included measurements of average β-amyloid peptide load and density of paired helical filament tau tangles across 8 brain regions (hippocampus, entorhinal cortex, midfrontal cortex, inferior temporal cortex, angular gyrus, calcarine cortex, anterior cingulate cortex, superior frontal cortex). Amyloid beta protein was identified by molecularly specific immunohistochemistry and quantified by image analysis. Neuronal neurofibrillary tangles were identified by molecularly specific immunohistochemistry (antibodies to abnormally phosphorylated Tau protein, AT8). As recommended by the ROS/MAP study authors, the square-root of the averages of β-amyloid load and tangle density was used in all analyses in our study. Post-mortem neuropathology data was available from 1694 individuals.

The global cognition score was calculated at each visit as the average of 19 tests assessing the individuals' episodic, working, and semantic memory, and perceptual orientation and speed. The raw score of each test were converted to Z scores and averaged to yield a global cognition score. The z-scores have a mean of 0 and standard deviation of 1. A negative z-score means that someone has a global cognition score lower than the cohort average at baseline. We used only the global cognition score

recorded at the subject's last recorded session before death for our analysis. Global cognition scores at the last visit before death were available from 1853 individuals.

Smoking status

The smoking status of the ROS/MAP participants was determined at the baseline interview by participants' answers to the following questions: 1. "Do you smoke cigarettes now?"; 2. "Did you ever smoke cigarettes regularly". Question 1 was used to determine current smokers, and question 2 identified former smokers. Participants who answered "no" to both questions were categorized as "never smoked".

Single-nucleus RNA sequencing and pre-processing

Details on the nucleus isolation and single nucleus RNA sequencing from the dorsolateral prefrontal cortex of 24 ROS/MAP individuals performed by Cain et al. 2020 are available on the Synapse AMP-AD Knowledge Portal (ID: syn16780177) and in the Cain et al. 2020 preprint. In brief, nuclei from an individual sample were loaded on a single channel on the 10x Genomics Chromium chip. Library construction was then performed as per the Chromium Single Cell 3' Reagent Kit v2 protocol (CG00052) provided by the manufacturer. The described protocol produces Illumina-ready sequencing libraries. All sequencing was performed on an Illumina HiSeq4000 machine. Generation of count files from the raw sequencing data was performed using the Cellranger software package (version 2.1.1, chemistry V2, 10X Genomics, for chemistry Single Cell 3'). For every nucleus, the number of genes for which at least one read was mapped was quantified, all nuclei with fewer than 400 detected genes were excluded.

Single-nucleus RNA sequencing data processing

The single-nucleus gene counts and metadata available from Cain et al. 2020 on synapse (ID: syn16780177) were converted into a Seurat object (37) in R Studio for further processing. Potential doublets were removed by filtering out cells with over 2500 detected features, and potential dead or dying cells were removed by excluding cells expressing over 5% mitochondrial genes. Cell type annotations were indicated in the data as described in the metadata downloaded from the Cain et al. 2020 Synapse repository (ID: syn16780177). The snRNAseq data was log-normalized and matched with genotype data (n = 22 individuals). *CHRNA5* expression was averaged per cell type per individual and *CHRNA5* levels in different cell types were then compared between cell types by one-way ANOVA with Tuckey's post-hoc t-test. To prevent bias for rare cell types in calculating average *CHRNA5* expression per cell type per individual, cell types with fewer than 100 individual cells represented in the original data (not aggregated) were removed (the layer 5 FEZF2 ET cell type was excluded from analysis as only 93 cells of this type were present in the genotype-matched snRNAseq dataset).

Gene ontology of chandelier cell genes

A set of genes which are upregulated in PVALB+ chandelier cells versus PVALB+ chandelier cells was previously generated by Bakken and colleagues (Bakken et. al. 2021, in their Supplementary table 20). From this list we first excluded all genes not specifically upregulated in humans (final n = 222) To determine the ontology of this gene set we used the Gene Ontology Resource (geneontology.org), searching specifically for molecular function.

Estimates of relative cell type proportions from bulk DLPFC RNAseq

153 Estimates of cell-type proportions from bulk DLPFC RNAseq data from 640 ROS/MAP participants was
154 performed and described by Cain et al. 2020. In brief: The authors developed a custom regression-based
155 consensus model, CelMod, to extract cell cluster specific genes from the snRNAseq dataset from 24
156 ROS/MAP participants, and then used these genes to estimate the proportions of different cell subtypes
157 in the bulk DLPFC RNAseq dataset from 640 ROS/MAP individuals. The deconvolved cell-type proportion
158 data from the DLPFC was available on request from the research group (Cain et al. 2020 personal
159 communication). We matched the cell type proportion data with genotype, bulk DLPFC RNAseq, and
160 neuropathology (brain levels of β-amyloid and tau) data (final n = 549 individuals). At the time of analysis
161 full cell-type annotations (like that in the snRNAseq data) were only available for the different classes of
162 inhibitory neuron proportions. The proportions of Inh.5, a PVALB+/LHX6+/THSD7A+ cell type, were
163 determined (Cain et al. 2020 personal communication) to represent chandelier cell proportions in DLPFC.

164 **Statistical approaches**

165 A detailed description of the statistical analyses is provided in **Supplement 1**.

166

167 **Results**

168 **Expression of α4β2α5 receptor component genes is affected by single nucleotide polymorphisms**

169 To identify effects in aging and dementia of gene variants previously shown in younger adults to
170 influence *CHRNA5* expression (33) and α5 coding (21,38), we examined brain expression quantitative
171 trait loci (eQTL). The variants were in weak-moderate linkage disequilibrium in our European ancestry
172 sample (r^2=0.34), in agreement with previous work (33). We also found that dosage of the A allele of the
173 missense SNP rs16969968 (minor allele frequency (MAF) = 0.33) in the coding region of *CHRNA5* (**Fig 1B**)
174 was associated with lower *CHRNA5* expression (t = -13.93 $p = 3.98*10^{-40}$), consistent with existing data
175 (39). A different SNP haplotype in the regulatory region upstream of *CHRNA5* (**Fig 1B**), denoted here by
176 the A allele of the tag SNP rs1979905 (MAF = 0.43), was associated with higher *CHRNA5* expression (t=
177 27.87, $p = 5.94*10^{-124}$) (**Fig. 1C**). Furthermore, analyses of the coding-SNP rs16969968 and the regulatory-
178 SNP rs1979905 together (**Fig. 1D**) showed that *CHRNA5* expression is predominantly regulated by the
179 regulatory-SNP rs1979905 rather than the coding-SNP, rs16969968, as all rs1979905 A allele non-carriers
180 showed similar levels of *CHRNA5* mRNA regardless of the rs16969968 A allele (Nested one-way ANOVA:
181 F(2) = 229.6; Šidák's post-hoc test for multiple comparisons: rs1979905 A1 vs. A0 $p = 8*10^{-6}$, A2 vs. A1 p =
182 0.004, A2 vs A0 $p = 4*10^{-6}$). This was also demonstrated using a conditional eQTL model, where the effect
183 of rs16969968 A allele on *CHRNA5* expression was lost when co-varying for rs1979905 A allele
184 (rs16969968A: t = -1.068, p = 0.2815; rs1979905A: t = 21.931, $p = 6.140*10^{-86}$). No trans-eQTL effects
185 were detected (**Fig. 1E**) between either of these SNPs and the expression of required partner nicotinic
186 subunit genes, *CHRNA4* and *CHRNB2*.

187 To assess the α4 and β2 nicotinic subunits required for the formation of α5-containing α4β2α5
188 receptors, we extended our eQTL analyses to SNPs in *CHRNA4* and *CHRNB2*, focusing on those associated
189 with altered gene expression or clinical effects(35,36,40). Without exception, eQTL SNP effects for these
190 genes were weaker than those of rs16969968 and rs1979905 for *CHRNA5*: the T allele of *CHRNB2*
191 intronic variant rs2072660 (MAF = 0.23) was associated with lower *CHRNB2* expression (t = -5, p =
192 $7.05*10^{-7}$), and a similar association with *CHRNB2* expression was seen with the T allele of the *CHRNB2*
193 non-coding variant rs4292956 (MAF = 0.07) (t = -5.244, $p = 2.02*10^{-7}$) (**Fig. 1E**). For *CHRNA4,* the G allele
194 of missense variant rs1044396 (MAF = 0.45) in the coding region of *CHRNA4* was associated with higher
195 *CHRNA4* expression (t = 3.67, p = 0.0003). We also used the Gene Query function of the xQTLServe online

196 tool (DLPFC of 534 ROS/MAP participants) to identify the T allele of the intronic variant rs45497800 as
197 associated with decreased *CHRNA4* expression (t = -6.92, $p = 1.32 * 10^{-11}$). We then replicated this
198 association in our larger cohort of 924 ROS/MAP individuals (MAF = 0.07) (t = -4.57, $p = 5.54*10^{-6}$) (**Fig.**
199 **1E**). No associations were found between these SNPs and the expression of other high-affinity nicotinic
200 receptor subunit genes (**Fig. 1E**).

201 ***CHRNA5* polymorphisms are not associated with smoking status in this largely nonsmoking population**

202 To investigate previously-reported (25,41) associations between genotype for the *CHRNA5* SNPs and
203 smoking status at baseline (current/former/never smoked), we used a Chi-squared test and found no
204 relationship (rs1979905_A : $\chi2(4) = 1.575$, p = 0.813; rs16969968_A: $\chi2(4) = 1.317$, p = 0.858) in this
205 largely nonsmoking population. Smoking status was not used in further analysis, unless specifically
206 indicated.

207 **A *CHRNA5* polymorphism is negatively associated with brain β-amyloid levels**

208 To address interrelationships among nicotinic subunit expression, nicotinic SNPs, and neuropathological
209 and cognitive phenotypes, we used clinical and post-mortem data in a multi-step model. As illustrated in
210 **Fig. 1F**, both β-amyloid and tau pathology were negatively associated with global cognitive performance
211 proximal to death (tau: t = -21 $p = 2.46*10^{-84}$; amyloid: t = -10.4, $p = -3.14*10^{-24}$) and positively associated
212 with each other (t = 17.68, $p = 6.96*10^{-63}$). Of the nicotinic receptor subunits and SNPs examined, only
213 the SNP increasing *CHRNA5* expression had a significant association with AD neuropathology, with the A
214 allele of the regulatory-SNP rs1979905 negatively associated with β-amyloid load (t = -2.551, $p = 0.011$).
215 This association remained significant after FDR correction ($p_{FDR} = 0.032$). By contrast, the expression of
216 the major nicotinic subunit genes *CHRNA4* and *CHRNB2* showed significant positive associations with the
217 last global cognition score, which remained significant after false discovery rate (FDR) correction for
218 multiple comparisons (*CHRNA4*: t = 2.98, $p_{FDR} = 0.01$; *CHRNB2*: t = 3.71, $p_{FDR} = 0.0009$). Conversely, the
219 rs2072660 T allele, associated with lower *CHRNB2* expression, was negatively associated with the last
220 global cognition score (t = -2.14, $p = 0.032$). A similar negative association with the last global cognition
221 score (t = -2.46, $p = 0.014$) was found for the T allele of the *CHRNB2* SNP rs4292956, and this association
222 remained significant after FDR correction ($p_{FDR} = 0.039$).

223 ***CHRNA5* expression does not tightly correlate with other components of the cholinergic system**

224 To further investigate the interrelationships among *CHRNA5* and the major nicotinic subunits as well as
225 other components of the cholinergic system, we performed a series of expression correlation analyses.
226 Most of the major components of the cholinergic system which were detected in bulk DLPFC data of the
227 ROS/MAP individuals (*CHRNA2*, *CHRNA4*, *CHRNA7*, *CHRNB2*, *CHRM3*, *CHRM1* and *ACHE*) showed
228 significant positive correlation with each other (**Fig. 1G**). By contrast, *CHRNA5* stood out as showing no
229 positive correlation with any of the other major cholinergic genes and only weak negative correlations
230 with the expression of *CHRNB2* and *CHRM1* (**Table 1**). Considering that the expression of *CHRNA5*,
231 *CHRNB2,* and *CHRNA4* are required for the assembly of the high-affinity α4β2α5 nicotinic receptor, it was
232 surprising to see that *CHRNA5* expression was not positively correlated with either *CHRNA4* or *CHRNB2*
233 (**Fig. 1G** and **Table 1**). Therefore, we next investigated whether this lack of correlation may arise from
234 differences in the cell-type specific expression of *CHRNA5* compared to the major nicotinic receptor
235 subunits, *CHRNA4* and *CHRNB2,* which are more broadly expressed.

236 ***CHRNA5* shows stronger expression in chandelier interneurons than most other cell classes**

237 To assess the cell-type specificity of *CHRNA5* expression in the ROS/MAP cohort, we calculated the
238 average *CHRNA5* expression per cell type per individual using the genotype-matched single-nucleus
239 RNAseq data available from the DLPFC in a subset of 22 ROS/MAP participants (31)(2 individuals lacked
240 genotyping data). In this small dataset, *CHRNA5* was expressed at a low level across a number of
241 different excitatory, inhibitory, and nonneuronal cell types (**Fig. 2A**), with significantly higher expression
242 in inhibitory PVALB+ chandelier cells (as identified by Cain et al. 2020). Chandelier cells had significantly-
243 higher expression of *CHRNA5* compared to most other cell types (One-way ANOVA: F(21) = 3.439, p =
244 $6.1*10^{-7}$; Tukey's post-hoc t-test Chandelier cells vs. 18 out of 19 other cell types: $p < 0.05$) (**Fig. 2A**). By
245 contrast, chandelier cell expression of *CHRNA4* and *CHRNB2* were at a similar level in chandelier cells to
246 their expression levels in many other cell types (**Fig. 2B**).

247 To confirm the novel finding that chandelier cells show stronger *CHRNA5* expression compared to other
248 classes of neurons, we probed publicly available cell-type specific gene expression databases of human
249 brain tissue. Using the Allen Institute SMART-seq single-cell transcriptomics data from multiple cortical
250 areas (https://celltypes.brain-map.org/rnaseq/human_ctx_smart-seq), we found *CHRNA5* expression to
251 be highest in a PVALB+/SCUBE3+ inhibitory cell type (0.06 trimmed mean *CHRNA5* expression) likely
252 representing chandelier cells (42), and in a co-clustering PVALB+/MFI+ cell type (0.06 trimmed mean
253 *CHRNA5* expression). In the Human Protein Atlas database (brain single cell tissue)
254 (https://www.proteinatlas.org/ENSG00000169684-CHRNA5/single+cell+type/brain), *CHRNA5* showed
255 highest expression in a PVALB+ inhibitory cell type (c-41) which also showed highest expression of
256 *SCUBE3* (Inhibitory neurons c-41, 15.1 normalized *CHRNA5* transcripts per million), likely also
257 representing chandelier cells.

258 To investigate the cell type-specificity of the *CHRNA5* eQTL effects of the regulatory-SNP rs1979905 in
259 the single nucleus data from ROS/MAP, we stratified the averaged *CHRNA5* expression by genotype for
260 the rs1979905 A allele. We found that higher allelic dosage of the rs1979905 A allele was associated with
261 greater *CHRNA5* expression (**Fig. 2C**), and that this pattern was most pronounced in subtypes of layer 5
262 (L5 RORB IT: t = 2.460, p = 0.0249) and layer 6 (L6 IT THEMIS: t = 2.402, p = 0.028) excitatory neurons
263 (**Fig. 2D**). In the stronger *CHRNA5*-expressing PVALB+ chandelier cells, however, the additive pattern did
264 not reach significance. Other neuronal cell types appeared to diverge completely from the typical eQTL
265 pattern of rs1979905 (**Fig. 2C,D**). This analysis suggests that only a subset of cell-types contribute to the
266 stepwise expression pattern observed in the prefrontal cortex by rs1979905 genotype.

267 Cell type specific data from ROS/MAP and the Allen database supports the hypothesis that *CHRNA5*
268 possesses a distinctive expression pattern with enrichment in chandelier cell interneurons, compared to
269 its more abundant and widely-expressed subunit partners.

270 **Chandelier cells are significantly enriched for genes interacting with β-amyloid**

271 To investigate the potential contribution of chandelier cells to β-amyloid processing, especially one that
272 might be driven by nicotinic α5-containing receptors, we assessed the molecular function of genes which
273 differentiate the chandelier cells from a different class of PVALB+ interneurons (basket cells). For this
274 analysis we took advantage of a list of 222 such genes previously generated by Bakken and colleagues
275 (30), who investigated the cellular identities of chandelier neurons in the cortex across species, including
276 humans. Apart from neurotransmission-associated molecular functions, molecular functional pathway
277 analysis revealed this list to be significantly enriched for genes defined as "amyloid-beta binding" (fold
278 enrichment = 7.79, p(FDR) = 0.01) (**Fig. 3A**), including *SORL1,* an endocytic receptor that directs the
279 amyloid precursor protein away from the amyloidogenic pathway (43–45) and *EPHA4,* a receptor
280 tyrosine kinase involved in amyloid regulation (46). Since α5-containing nicotinic receptors are highly
281 permeable to calcium ions (21,22), we note that chandelier neurons are also significantly enriched for

genes with a "calcium ion binding" molecular function (fold enrichment = 3.77, *p*(FDR) = $4.12*10^{-6}$) (**Fig. 3B)**, including genes potentially protective against amyloid pathology such as *MME and SPOCK1*. Two genes are at the intersection of these functional pathways in chandelier cells, *PRNP and CLSTN2*. The former has been implicated in nicotinic receptor-mediated regulation of amyloid (47–50) and the latter is essential for normal cortical levels of GABAergic neurotransmission (51) These findings underscore the importance of investigating the relationship between the functional status of nicotinic α5 subunits and chandelier neuron vulnerability to AD neuropathology.

A genotype-specific reduction in proportion of chandelier cells with increasing brain β-amyloid levels

To determine whether impaired function/trafficking α5-containing nicotinic receptors might promote chandelier neuron vulnerability to neurodegeneration, we examined the interaction of rs16969968 genotype and AD neuropathology on estimated proportions of chandelier neurons in the bulk RNAseq dataset. This investigation was based on cell type proportion estimates for chandelier cells and several other interneuron subclasses, from sets of single-cell-informed marker genes, in a subset of 640 ROS/MAP participants Overall, β-amyloid levels were negatively associated with the proportion of chandelier cells (t = -4.024, $p = 7*10^{-5}$). However, the missense rs16969968 A allele homozygotes showed significantly lower chandelier cell proportions with increasing β-amyloid load (**Fig. 4A**), compared to rs16969968 A allele non-carriers (interaction term t = -2.799, *p* = 0.005)(**Fig. 4B)**. In a secondary analysis, a near-significant positive association of rs1979905 A allele and β-amyloid levels with chandelier cells was observed (**Fig. 4C**), with rs1979905 A allele homozygotes showing a trend towards a smaller drop in chandelier cell proportions with increasing β-amyloid, compared to rs1979905 A allele non-carriers (interaction term t = 1.769, *p* = 0.078)(**Fig. 4D**). The observed relationships between chandelier cell proportions, *CHRNA5* genotypes and amyloid were not altered by the inclusion of smoking status as a covariate in the analysis. Chandelier cell proportions did not correlate with tau pathology (t = -0.307, *p* = 0.759), nor was there an interaction of *CHRNA5* genotype and tau pathology with chandelier cell proportions (data not shown).

To assess whether the interaction between β-amyloid levels and *CHRNA5* SNPs was driven by the effects of these SNPs on *CHRNA5* expression, we assessed the effect of the interaction of *CHRNA5* levels and β-amyloid load on chandelier cell proportion but found no significant effect (t = 2.711, p = 0.544). This suggests that the genotype-specific association between amyloid load and chandelier cell proportion is more likely driven by changes in nicotinic α5 protein structure and/or trafficking (52) as a consequence of having two copies of the missense SNP in *CHRNA5*.

The schematic in **Fig. 5** illustrates a working model of the impact of the rs16969968 A allele homozygosity for chandelier cell vulnerability, as well as example mechanisms enriched in chandelier cells and known to alter β-amyloid processing.

Discussion

We examined human prefrontal cortical *CHRNA5* expression in aging, probing the connections between SNPs affecting the expression and function/trafficking of the nicotinic α5 subunit gene and AD-related neuropathology. The aging prefrontal cortex demonstrates strong eQTL effects of the regulatory-SNP rs1979905, and we show that the A allele of rs1979905 is associated with lower levels of brain β-amyloid. Single-nucleus RNAseq data revealed that chandelier cells have the greatest abundance of *CHRNA5* in human prefrontal cortex. These neurons are significantly enriched in amyloid-binding

proteins, including some that may be activated via nicotinic receptors. Lastly, we examined the impact of AD neuropathology on the proportions of chandelier neurons and determined that the α5-altering coding-SNP rs16969968 renders this interneuron population vulnerable to β-amyloid levels. Our findings, summarized in the working model in **Fig 5**, suggest a potential cell-type specific neuroprotective role for C*HRNA5* to reduce β-amyloid levels and toxicity.

Inhibitory signalling is disrupted in Alzheimer's disease

The disruption of the excitatory/inhibitory balance in the cortex is a hallmark of AD pathology and is associated with cognitive AD symptoms (3,4). Previous studies have shown disruption of cortical inhibitory signalling in AD stems from the alteration of the activity of inhibitory neurons and inhibitory cell loss (53–55). The susceptibility of inhibitory neurons to AD pathology is not uniform, however. While studies have shown significant drops in somatostatin-positive interneurons in the cortex of AD patients (56,57), the numbers of parvalbumin-positive cortical interneurons, including the PVALB+ chandelier cells, appear comparatively more resilient to AD pathology (57,58). Our study expands on these findings, demonstrating that the preservation of chandelier cells in AD pathology depends on the genotype of SNP in a nicotinic receptor subunit. The rs16969968 SNP is a missense mutation found to functionally alter the α5-containing nicotinic receptors in cell systems and *in vivo*, through altered channel biosynthesis, trafficking, properties and/or modulation (21,38,52,59,60). Recent optophysiological work suggests that the nicotinic α5 subunit accelerates the endogenous cholinergic response in prefrontal cortex and protects it against desensitization (20), but little is known about endogenous cholinergic modulation of chandelier neurons.

Chandelier cells are vulnerable to β-amyloid pathology

Chandelier cells are a specialized subtype of PVALB+ interneurons. They differ anatomically from the PVALB+ basket cells by their large number of vertically oriented axonal cartridges, which specifically innervate the axon initial segments of pyramidal neurons (61,62). New evidence suggests chandelier cells regulate excitation dynamics of neuronal networks (63). Impairment of these neurons has been implicated in diseases involving pathological excitation in the cortex, such as epilepsy (64,65) and AD (3,4,58). Our RNASeq findings are in agreement with previous work showing that the inhibitory output of chandelier cells is sensitive to β-amyloid pathology (66) but unaffected by tau pathology (67). Chandelier cell axons near β-amyloid plaques have been found to show deformations, and pyramidal neurons proximal to plaques show loss of inhibitory input onto their axon initial segments (66). Our findings suggest that in people homozygous for A allele of the missense *CHRNA5* SNP rs16969968, this vulnerability of chandelier cells to β-amyloid pathology may be exacerbated, possibly leading to cell death.

Potential mechanisms for a neuroprotective effect of α5-containing nicotinic receptors

Our results suggest that polymorphisms affecting *CHRNA5* expression and function, may alter both the total β-amyloid levels in the brain, and alter the susceptibility of specific *CHRNA5*-expressing cell types, such as the chandelier cells, to β-amyloid-mediated toxicity. One possible explanation for these observations may be the lowered binding of β-amyloid to the α4β2α5 nicotinic receptors (Lamb et al. 2005) expressed by these cells. This protection against β-amyloid binding and inhibition of the nicotinic response (12) could promote resilience of nicotinic signalling in the chandelier cells, potentially leading to improved cell survival (14) in AD pathology. Furthermore, since α4β2α5 nicotinic receptors support higher conductance of calcium ions into the cell (21,22), another putative neuroprotective mechanism of

367 the α5 subunit may be through driving possible calcium-dependent neuroprotective pathways in the
368 neurons which express the α4β2α5 nicotinic receptors (68,69). Such calcium-regulated pathways may
369 include *MME*, *SORL1*, *SPOCK1* or *PRNP*, which are specifically enriched in PVALB+ chandelier cells
370 compared to PVALB+ non-chandelier cells (30), and which have been previously suggested to alter β-
371 amyloid production and clearance (44,47,48,70).

372 **Caveats and opportunities for additional investigation**

373 While the ROS/MAP database offered an opportunity to assess the impact of *CHRNA5* expression and
374 *CHRNA5*-related SNPs on AD pathology in a large sample, some caveats exist. As *CHRNA5* expression has
375 previously been shown to be important for animal performance in demanding attentional tasks (23,24),
376 one of the critical limitations of our study is that a robust attention assessment of the ROS/MAP
377 individuals was not part of the study design. While the ROS/MAP dataset presented an opportunity to
378 study the effects of rs16969968 on a background of an unusually-low smoking prevalence (71), future
379 work would benefit from more robust assessment of smoking history.

380 A limitation of the single-nucleus RNA sequencing data (31) was its relatively low number of individuals,
381 limiting the robustness of comparing the effects of rs1979905 on *CHRNA5* expression across the
382 different cell types, and preventing a similar examination of cell-type specific effects of rs16969968
383 on *CHRNA5* expression.

384 Since cortical cell-type proportions were estimated using patterns of marker gene expression (31), the
385 decreased chandelier cell proportions may instead reflect reductions of chandelier cell cartridges in AD
386 (58). While the disruption of cortical E/I balance would remain similar, a different interpretation of our
387 data would be that the rs16969968 A allele homozygous genotype exacerbates chandelier cartridge loss
388 in AD, reducing their functional output, and resulting in lower expression of chandelier-cell-specific
389 marker genes in individuals with elevated β-amyloid.

390 Finally, RNA sequencing data may not fully capture the protein-level changes in AD brains (72). This
391 limitation should be considered when interpreting the findings of our study.

392 **Summary and implications**

393 A growing body of work suggests that cortical excitability is perturbed early in Alzheimer's disease
394 through impairment of inhibitory interneurons (53,73). *CHRNA5* is positioned to modulate the overall
395 excitability of the prefrontal cortex in two ways: through the excitation of a population of deep layer
396 cortical pyramidal neurons (20,74,75) that send projections throughout prefrontal cortex and, as
397 ascertained from our findings in this study, through the excitation of specific subsets of cortical
398 interneurons, the chandelier cells. Our findings suggest that *CHRNA5* is involved in Alzheimer's disease
399 neuropathology. The A allele of the *CHRNA5* regulatory-SNP rs1979905 is associated with higher
400 expression of *CHRNA5* and with reduced β-amyloid load in the brain. In parallel, the A allele of the
401 missense SNP, rs16969968, is associated with fewer chandelier cells in individuals with high β-amyloid
402 levels, suggesting that differences in the protein structure of *CHRNA5* contributes cellular resiliency to β-
403 amyloid pathology. This combination suggests neuroprotective roles of *CHRNA5* in β-amyloid pathology
404 and makes *CHRNA5* a target for therapies aiming to improve neuron survival in Alzheimer's disease.

405

406 **References**

407 1. Hampel H, Mesulam M-M, Cuello AC, Farlow MR, Giacobini E, Grossberg GT, et al. The cholinergic
408 system in the pathophysiology and treatment of Alzheimer's disease. Brain. 2018 Jul
409 1;141(7):1917–33. Available from: https://pubmed.ncbi.nlm.nih.gov/29850777

410 2. Busche MA, Hyman BT. Synergy between amyloid-β and tau in Alzheimer's disease. Nat Neurosci.
411 2020;23(10):1183–93. Available from: https://doi.org/10.1038/s41593-020-0687-6

412 3. Lauterborn JC, Scaduto P, Cox CD, Schulmann A, Lynch G, Gall CM, et al. Increased excitatory to
413 inhibitory synaptic ratio in parietal cortex samples from individuals with Alzheimer's disease. Nat
414 Commun. 2021;12(1):2603. Available from: https://doi.org/10.1038/s41467-021-22742-8

415 4. Vico Varela E, Etter G, Williams S. Excitatory-inhibitory imbalance in Alzheimer's disease and
416 therapeutic significance. Neurobiol Dis. 2019;127:605–15. Available from:
417 https://www.sciencedirect.com/science/article/pii/S0969996118307599

418 5. Pafundo DE, Miyamae T, Lewis DA, Gonzalez-Burgos G. Cholinergic modulation of neuronal
419 excitability and recurrent excitation-inhibition in prefrontal cortex circuits:
420 implications for gamma oscillations. J Physiol. 2013/07/01. 2013 Oct
421 1;591(19):4725–48. Available from:
422 https://pubmed.ncbi.nlm.nih.gov/23818693

423 6. Obermayer J, Luchicchi A, Heistek TS, de Kloet SF, Terra H, Bruinsma B, et al.
424 Prefrontal cortical ChAT-VIP interneurons provide local excitation by
425 cholinergic synaptic transmission and control attention. Nat Commun. 2019;10(1):5280. Available
426 from: https://doi.org/10.1038/s41467-019-13244-9

427 7. Bartus RT, Dean RL, Beer B, Lippa AS. The Cholinergic Hypothesis of Geriatric Memory
428 Dysfunction. Science (80-). 1982 Jul 30;217(4558):408–14. Available from:
429 https://doi.org/10.1126/science.7046051

430 8. Court J, Martin-Ruiz C, Piggott M, Spurden D, Griffiths M, Perry E. Nicotinic receptor abnormalities
431 in Alzheimer's disease. Biol Psychiatry. 2001;49(3):175–84. Available from:
432 https://www.sciencedirect.com/science/article/pii/S0006322300011161

433 9. Nordberg A, Winblad B. Reduced number of [3H]nicotine and [3H]acetylcholine binding sites in
434 the frontal cortex of Alzheimer brains. Neurosci Lett. 1986 Dec;72(1):115–9.

435 10. Lasala M, Fabiani C, Corradi J, Antollini S, Bouzat C. Molecular Modulation of Human α7 Nicotinic
436 Receptor by Amyloid-β Peptides. Front Cell Neurosci. 2019;13. Available from:
437 https://www.frontiersin.org/article/10.3389/fncel.2019.00037

438 11. Buckingham SD, Jones AK, Brown LA, Sattelle DB. Nicotinic acetylcholine receptor signalling: roles
439 in Alzheimer's disease and amyloid neuroprotection. Pharmacol Rev. 2009 Mar;61(1):39–61.

440 12. Wu J, Kuo Y-P, George AA, Xu L, Hu J, Lukas RJ. beta-Amyloid directly inhibits human alpha4beta2-
441 nicotinic acetylcholine receptors heterologously expressed in human SH-EP1 cells. J Biol Chem.
442 2004 Sep;279(36):37842–51.

443 13. Lamb PW, Melton MA, Yakel JL. Inhibition of neuronal nicotinic acetylcholine receptor channels
444 expressed in Xenopus oocytes by beta-amyloid1-42 peptide. J Mol Neurosci. 2005;27(1):13–21.

445 14. Kihara T, Shimohama S, Sawada H, Kimura J, Kume T, Kochiyama H, et al. Nicotinic receptor
446 stimulation protects neurons against beta-amyloid toxicity. Ann Neurol. 1997 Aug;42(2):159–63.

447 15. He N, Wang Z, Wang Y, Shen H, Yin M. ZY-1, A Novel Nicotinic Analog, Promotes Proliferation and
448 Migration of Adult Hippocampal Neural Stem/Progenitor Cells. Cell Mol Neurobiol.
449 2013;33(8):1149–57. Available from: https://doi.org/10.1007/s10571-013-9981-0

450 16. Nie H, Wang Z, Zhao W, Lu J, Zhang C, Lok K, et al. New nicotinic analogue ZY-1 enhances
451 cognitive functions in a transgenic mice model of Alzheimer's disease. Neurosci Lett.
452 2013;537:29–34. Available from:
453 https://www.sciencedirect.com/science/article/pii/S0304394013000153

454 17. Deardorff WJ, Feen E, Grossberg GT. The Use of Cholinesterase Inhibitors Across All Stages of
455 Alzheimer's Disease. Drugs Aging. 2015;32(7):537–47. Available from:
456 https://doi.org/10.1007/s40266-015-0273-x

457 18. Albuquerque EX, Pereira EFR, Alkondon M, Rogers SW. Mammalian Nicotinic Acetylcholine
458 Receptors: From Structure to Function. Physiol Rev. 2009;89(1):73–120. Available from:
459 https://doi.org/10.1152/physrev.00015.2008

460 19. Ramirez-Latorre J, Yu CR, Qu X, Perin F, Karlin A, Role L. Functional contributions of α5 subunit to
461 neuronal acetylcholine receptor channels. Nature. 1996;380(6572):347–51. Available from:
462 https://doi.org/10.1038/380347a0

463 20. Venkatesan S, Lambe EK. Chrna5 is essential for a rapid and protected response to optogenetic
464 release of endogenous acetylcholine in prefrontal cortex. J Neurosci. 2020;40(38).

465 21. Sciaccaluga M, Monconi C, Martinello K, Catalano M, Bermudez I, Stitzel JA, et al. Crucial role of
466 nicotinic α5 subunit variants for Ca2+ fluxes in ventral midbrain neurons. FASEB J.
467 2015;29(8):3389–98. Available from:
468 https://faseb.onlinelibrary.wiley.com/doi/abs/10.1096/fj.14-268102

469 22. Scholze P, Huck S. The α5 Nicotinic Acetylcholine Receptor Subunit Differentially Modulates
470 α4β2* and α3β4* Receptors. Front Synaptic Neurosci. 2020;12. Available from:
471 https://www.frontiersin.org/article/10.3389/fnsyn.2020.607959

472 23. Bailey CDC, De Biasi M, Fletcher PJ, Lambe EK. The Nicotinic Acetylcholine Receptor α5 Subunit
473 Plays a Key Role in Attention Circuitry and Accuracy. J Neurosci. 2010 Jul 7;30(27):9241 LP – 9252.
474 Available from: http://www.jneurosci.org/content/30/27/9241.abstract

475 24. Howe WM, Brooks JL, Tierney PL, Pang J, Rossi A, Young D, et al. α5 nAChR modulation of the
476 prefrontal cortex makes attention resilient. Brain Struct Funct. 2018 Mar;223(2):1035–47.

477 25. Schuch JB, Polina ER, Rovaris DL, Kappel DB, Mota NR, Cupertino RB, et al. Pleiotropic effects of
478 Chr15q25 nicotinic gene cluster and the relationship between smoking, cognition and ADHD. J
479 Psychiatr Res. 2016 Sep;80:73–8.

480 26. Han W, Zhang T, Ni T, Zhu L, Liu D, Chen G, et al. Relationship of common variants in CHRNA5 with
481 early-onset schizophrenia and executive function. Schizophr Res. 2019 Apr;206:407–12.

482 27. Jensen KP, DeVito EE, Herman AI, Valentine GW, Gelernter J, Sofuoglu M. A CHRNA5 Smoking Risk
483 Variant Decreases the Aversive Effects of Nicotine in Humans. Neuropsychopharmacology.
484 2015/05/07. 2015 Nov;40(12):2813–21. Available from:
485 https://pubmed.ncbi.nlm.nih.gov/25948103

486 28. Livingston G, Huntley J, Sommerlad A, Ames D, Ballard C, Banerjee S, et al. Dementia prevention,
487 intervention, and care: 2020 report of the Lancet Commission. Lancet. 2020 Aug

488 8;396(10248):413–46. Available from: https://doi.org/10.1016/S0140-6736(20)30367-6

489 29. Bennett DA, Buchman AS, Boyle PA, Barnes LL, Wilson RS, Schneider JA. Religious Orders Study
490 and Rush Memory and Aging Project. J Alzheimers Dis. 2018;64(s1):S161–89.

491 30. Bakken TE, Jorstad NL, Hu Q, Lake BB, Tian W, Kalmbach BE, et al. Comparative cellular analysis of
492 motor cortex in human, marmoset and mouse. Nature. 2021;598(7879):111–9. Available from:
493 https://doi.org/10.1038/s41586-021-03465-8

494 31. Cain A, Taga M, McCabe C, Hekselman I, White CC, Green G, et al. Multi-cellular communities are
495 perturbed in the aging human brain and with Alzheimer's disease. bioRxiv. 2020; Available from:
496 https://www.biorxiv.org/content/early/2020/12/23/2020.12.22.424084

497 32. Ji X, Gui J, Han Y, Brennan P, Li Y, McKay J, et al. The role of haplotype in 15q25.1 locus in lung
498 cancer risk: results of scanning chromosome 15. Carcinogenesis. 2015 Nov;36(11):1275–83.

499 33. Smith RM, Alachkar H, Papp AC, Wang D, Mash DC, Wang J-C, et al. Nicotinic α5 receptor subunit
500 mRNA expression is associated with distant 5′ upstream polymorphisms. Eur J Hum Genet.
501 2011;19(1):76–83. Available from: https://doi.org/10.1038/ejhg.2010.120

502 34. Wessel J, McDonald SM, Hinds DA, Stokowski RP, Javitz HS, Kennemer M, et al. Resequencing of
503 nicotinic acetylcholine receptor genes and association of common and rare variants with the
504 Fagerström test for nicotine dependence. Neuropsychopharmacology. 2010/08/25. 2010
505 Nov;35(12):2392–402. Available from: https://pubmed.ncbi.nlm.nih.gov/20736995

506 35. Swan GE, Javitz HS, Jack LM, Wessel J, Michel M, Hinds DA, et al. Varenicline for smoking
507 cessation: nausea severity and variation in nicotinic receptor genes. Pharmacogenomics J.
508 2012;12(4):349–58. Available from: https://doi.org/10.1038/tpj.2011.19

509 36. Sadaghiani S, Ng B, Altmann A, Poline J-B, Banaschewski T, Bokde ALW, et al. Overdominant Effect
510 of a CHRNA4 Polymorphism on Cingulo-Opercular Network Activity and Cognitive Control. J
511 Neurosci. 2017;37(40):9657–66. Available from: https://www.jneurosci.org/content/37/40/9657

512 37. Satija R, Farrell JA, Gennert D, Schier AF, Regev A. Spatial reconstruction of single-cell gene
513 expression data. Nat Biotechnol. 2015;33(5):495–502. Available from:
514 https://doi.org/10.1038/nbt.3192

515 38. Kuryatov A, Berrettini W, Lindstrom J. Acetylcholine receptor (AChR) α5 subunit variant
516 associated with risk for nicotine dependence and lung cancer reduces $(\alpha4\beta2)_2\alpha5$ AChR function.
517 Mol Pharmacol. 2011 Jan;79(1):119–25.

518 39. Wang J-C, Spiegel N, Bertelsen S, Le N, McKenna N, Budde JP, et al. Cis-Regulatory Variants Affect
519 CHRNA5 mRNA Expression in Populations of African and European Ancestry. PLoS One. 2013 Nov
520 26;8(11):e80204. Available from: https://doi.org/10.1371/journal.pone.0080204

521 40. Hoft NR, Stitzel JA, Hutchison KE, Ehringer MA. CHRNB2 promoter region: association with
522 subjective effects to nicotine and gene expression differences. Genes Brain Behav. 2010/11/04.
523 2011 Mar;10(2):176–85. Available from: https://pubmed.ncbi.nlm.nih.gov/20854418

524 41. Jensen KP, Devito EE, Herman AI, Valentine GW, Gelernter J, Sofuoglu M. A CHRNA5 smoking risk
525 variant decreases the aversive effects of nicotine in humans. Neuropsychopharmacology.
526 2015;40(12):2813–21.

527 42. Hodge RD, Bakken TE, Miller JA, Smith KA, Barkan ER, Graybuck LT, et al. Conserved cell types
528 with divergent features in human versus mouse cortex. Nature. 2019 Sep;573(7772):61–8.

529 43. Andersen OM, Reiche J, Schmidt V, Gotthardt M, Spoelgen R, Behlke J, et al. Neuronal sorting
530 protein-related receptor sorLA/LR11 regulates processing of the amyloid precursor protein. Proc
531 Natl Acad Sci. 2005;102(38):13461–6. Available from:
532 https://www.pnas.org/doi/abs/10.1073/pnas.0503689102

533 44. Caglayan S, Takagi-Niidome S, Liao F, Carlo A-S, Schmidt V, Burgert T, et al. Lysosomal Sorting of
534 Amyloid-β by the SORLA Receptor Is Impaired by a Familial Alzheimer's Disease Mutation. Sci
535 Transl Med. 2014;6(223):223ra20-223ra20. Available from:
536 https://www.science.org/doi/abs/10.1126/scitranslmed.3007747

537 45. Hung C, Tuck E, Stubbs V, van der Lee SJ, Aalfs C, van Spaendonk R, et al. SORL1 deficiency in
538 human excitatory neurons causes APP-dependent defects in the endolysosome-autophagy
539 network. Cell Rep. 2021;35(11):109259. Available from:
540 https://www.sciencedirect.com/science/article/pii/S2211124721006239

541 46. Tamura K, Chiu Y-W, Shiohara A, Hori Y, Tomita T. EphA4 regulates Aβ production via BACE1
542 expression in neurons. FASEB J Off Publ Fed Am Soc Exp Biol. 2020 Dec;34(12):16383–96.

543 47. Griffiths HH, Whitehouse IJ, Hooper NM. Regulation of amyloid-β production by the prion protein.
544 Prion. 2012/07/01. 2012 Jul 1;6(3):217–22. Available from:
545 https://pubmed.ncbi.nlm.nih.gov/22449984

546 48. Nie H, Li Z, Lukas RJ, Shen Y, Song L, Wang X, et al. Construction of SH-EP1-alpha4beta2-hAPP695
547 cell line and effects of nicotinic agonists on beta-amyloid in the cells. Cell Mol Neurobiol. 2008
548 Jan;28(1):103–12.

549 49. Beraldo FH, Arantes CP, Santos TG, Queiroz NGT, Young K, Rylett RJ, et al. Role of alpha7 nicotinic
550 acetylcholine receptor in calcium signaling induced by prion protein interaction with stress-
551 inducible protein 1. J Biol Chem. 2010 Nov;285(47):36542–50.

552 50. Nygaard HB, Strittmatter SM. Cellular Prion Protein Mediates the Toxicity of β-Amyloid
553 Oligomers: Implications for Alzheimer Disease. Arch Neurol. 2009;66(11):1325–8. Available from:
554 https://doi.org/10.1001/archneurol.2009.223

555 51. Lipina T V, Prasad T, Yokomaku D, Luo L, Connor SA, Kawabe H, et al. Cognitive Deficits in
556 Calsyntenin-2-deficient Mice Associated with Reduced GABAergic Transmission.
557 Neuropsychopharmacol Off Publ Am Coll Neuropsychopharmacol. 2016 Feb;41(3):802–10.

558 52. Maskos U. The nicotinic receptor alpha5 coding polymorphism rs16969968 as a major target in
559 disease: Functional dissection and remaining challenges. J Neurochem. 2020;154(3):241–50.
560 Available from: https://onlinelibrary.wiley.com/doi/abs/10.1111/jnc.14989

561 53. Hijazi S, Heistek TS, Scheltens P, Neumann U, Shimshek DR, Mansvelder HD, et al. Early
562 restoration of parvalbumin interneuron activity prevents memory loss and network
563 hyperexcitability in a mouse model of Alzheimer's disease. Mol Psychiatry. 2020;25(12):3380–98.
564 Available from: https://doi.org/10.1038/s41380-019-0483-4

565 54. Wright AL, Zinn R, Hohensinn B, Konen LM, Beynon SB, Tan RP, et al. Neuroinflammation and
566 neuronal loss precede Aβ plaque deposition in the hAPP-J20 mouse model of Alzheimer's
567 disease. PLoS One. 2013;8(4):e59586.

568 55. Zheng J, Li H-L, Tian N, Liu F, Wang L, Yin Y, et al. Interneuron Accumulation of Phosphorylated tau
569 Impairs Adult Hippocampal Neurogenesis by Suppressing GABAergic Transmission. Cell Stem Cell.
570 2020 Mar 5;26(3):331-345.e6. Available from: https://doi.org/10.1016/j.stem.2019.12.015

571 56. Beal MF, Mazurek MF, Svendsen CN, Bird ED, Martin JB. Widespread reduction of somatostatin-
572 like immunoreactivity in the cerebral cortex in Alzheimer's disease. Ann Neurol. 1986
573 Oct;20(4):489–95.

574 57. Waller R, Mandeya M, Viney E, Simpson JE, Wharton SB. Histological characterization of
575 interneurons in Alzheimer's disease reveals a loss of somatostatin interneurons in the temporal
576 cortex. Neuropathology. 2020 Aug;40(4):336–46.

577 58. Fonseca M, Soriano E, Ferrer I, Martinez A, Tun˜on T. Chandelier cell axons identified by
578 parvalbumin-immunoreactivity in the normal human temporal cortex and in Alzheimer's disease.
579 Neuroscience. 1993;55(4):1107–16. Available from:
580 https://www.sciencedirect.com/science/article/pii/0306452293903249

581 59. Koukouli F, Rooy M, Tziotis D, Sailor KA, O'Neill HC, Levenga J, et al. Nicotine reverses
582 hypofrontality in animal models of addiction and schizophrenia. Nat Med. 2017;23(3):347–54.
583 Available from: https://doi.org/10.1038/nm.4274

584 60. Forget B, Scholze P, Langa F, Morel C, Pons S, Mondoloni S, et al. A Human Polymorphism in
585 CHRNA5 Is Linked to Relapse to Nicotine Seeking in Transgenic Rats. Curr Biol. 2018;28(20):3244-
586 3253.e7. Available from: https://www.sciencedirect.com/science/article/pii/S096098221831128X

587 61. Fairén A, Valverde F. A specialized type of neuron in the visual cortex of cat: a Golgi and electron
588 microscope study of chandelier cells. J Comp Neurol. 1980 Dec;194(4):761–79.

589 62. Somogyi P. A specific "axo-axonal" interneuron in the visual cortex of the rat. Brain Res. 1977
590 Nov;136(2):345–50.

591 63. Schneider-Mizell CM, Bodor AL, Collman F, Brittain D, Bleckert A, Dorkenwald S, et al. Structure
592 and function of axo-axonic inhibition. Calabrese RL, Callaway E, Huang ZJ, Oberlaender M, editors.
593 Elife. 2021;10:e73783. Available from: https://doi.org/10.7554/eLife.73783

594 64. Ribak CE. Axon terminals of GABAergic chandelier cells are lost at epileptic foci. Brain Res.
595 1985;326(2):251–60. Available from:
596 https://www.sciencedirect.com/science/article/pii/0006899385900344

597 65. Zhu Y, Stornetta RL, Zhu JJ. Chandelier Cells Control Excessive Cortical Excitation: Characteristics
598 of Whisker-Evoked Synaptic Responses of Layer 2/3 Nonpyramidal and Pyramidal Neurons. J
599 Neurosci. 2004 Jun 2;24(22):5101 LP – 5108. Available from:
600 http://www.jneurosci.org/content/24/22/5101.abstract

601 66. León-Espinosa G, DeFelipe J, Muñoz A. Effects of amyloid-β plaque proximity on the axon initial
602 segment of pyramidal cells. J Alzheimers Dis. 2012;29(4):841–52.

603 67. Blazquez-Llorca L, Garcia-Marin V, Defelipe J. Pericellular innervation of neurons expressing
604 abnormally hyperphosphorylated tau in the hippocampal formation of Alzheimer's disease
605 patients. Front Neuroanat. 2010;4:20.

606 68. Ueda M, Iida Y, Kitamura Y, Kawashima H, Ogawa M, Magata Y, et al. 5-Iodo-A-85380, a specific
607 ligand for alpha 4 beta 2 nicotinic acetylcholine receptors, prevents glutamate neurotoxicity in
608 rat cortical cultured neurons. Brain Res. 2008 Mar;1199:46–52.

609 69. Cingir Koker S, Jahja E, Shehwana H, Keskus AG, Konu O. Cholinergic Receptor Nicotinic Alpha 5
610 (CHRNA5) RNAi is associated with cell cycle inhibition, apoptosis, DNA damage response and drug
611 sensitivity in breast cancer. PLoS One. 2018;13(12):e0208982.

612 70. Barrera-Ocampo A, Arlt S, Matschke J, Hartmann U, Puig B, Ferrer I, et al. Amyloid-β Precursor
613 Protein Modulates the Sorting of Testican-1 and Contributes to Its Accumulation in Brain Tissue
614 and Cerebrospinal Fluid from Patients with Alzheimer Disease. J Neuropathol Exp Neurol. 2016
615 Sep 1;75(9):903–16. Available from: https://doi.org/10.1093/jnen/nlw065

616 71. Cornelius ME, Loretan CG, Wang TW, Jamal A, Moma DM. Tobacco Product Use Among Adults —
617 United States, 2020. MMWR Morb Mortal Wkly Rep. 2022;71:397–405.

618 72. Johnson ECB, Carter EK, Dammer EB, Duong DM, Gerasimov ES, Liu Y, et al. Large-scale deep
619 multi-layer analysis of Alzheimer's disease brain reveals strong proteomic disease-related changes
620 not observed at the RNA level. Nat Neurosci. 2022;25(2):213–25. Available from:
621 https://doi.org/10.1038/s41593-021-00999-y

622 73. Petrache AL, Rajulawalla A, Shi A, Wetzel A, Saito T, Saido TC, et al. Aberrant Excitatory-Inhibitory
623 Synaptic Mechanisms in Entorhinal Cortex Microcircuits During the Pathogenesis of Alzheimer's
624 Disease. Cereb Cortex. 2019 Apr 1;29(4):1834–50. Available from:
625 https://pubmed.ncbi.nlm.nih.gov/30766992

626 74. Wada E, McKinnon D, Heinemann S, Patrick J, Swanson LW. The distribution of mRNA encoded by
627 a new member of the neuronal nicotinic acetylcholine receptor gene family (alpha 5) in the rat
628 central nervous system. Brain Res. 1990 Aug;526(1):45–53.

629 75. Winzer-Serhan UH, Leslie FM. Expression of alpha5 nicotinic acetylcholine receptor subunit mRNA
630 during hippocampal and cortical development. J Comp Neurol. 2005 Jan;481(1):19–30.

631

632

633 **Figure legends**

634 **Figure 1. SNPs affecting expression of α4β2* nicotinic receptor subunit genes highlight a link between**
635 ***CHRNA5* and amyloid pathology. *A,*** Schematics illustrating different subunit compositions of prefrontal
636 α4β2* nicotinic receptors, with and without the α5 subunit. ***B,*** Localization of the rs16969968 and
637 rs1979905 SNPs in relation to the *CHRNA5* locus. ***C,*** The A allele of the missense SNP rs16969968 (left) in
638 the coding region of *CHRNA5* is associated with lowered *CHRNA5* expression, while the A allele of the
639 rs1979905 SNP (middle) upstream of the *CHRNA5* gene is associated with enhanced *CHRNA5* expression.
640 Data from the DLPFC of ROS/MAP individuals. ***D,*** *CHRNA5* expression appears to be controlled by the
641 zygosity of the rs1979905 A allele (colors) instead of the rs16969968 A allele (x-axis). Data shown as
642 *CHRNA5* expression for each subject with means indicated. ***E,*** eQTL effects of SNPs in nicotinic subunit
643 genes on their respective gene expression. Shown as β-coefficient with significance (p) in brackets. **F,**
644 Network plot depicting the relationships between SNPs (black), gene expression (red), neuropathology
645 (blue), and last global cognition score (green). Only associations $p < 0.05$ before adjustment for false
646 discovery rate (FDR) are indicated in the plot. Solid and dashed lines indicate whether association was
647 significant after correction for FDR or not, respectively. **G,** Network plot depicting the correlations
648 present between the expression of select cholinergic genes in the DLPFC. Colour of lines indicates
649 direction of correlation (negative or positive) while the thickness indicates correlation strength. All
650 correlations shown are significant after adjustment for FDR.

651 **Figure 2. *CHRNA5* expression is elevated in chandelier cells and is affected by genotype for the**
652 **rs1979905 A allele. *A,*** Expression of *CHRNA5* averaged per cell type per individual, original gene count
653 values were normalized for each cell by total expression. F-test significance of ANOVA shown on graph,
654 with red asterisk denoting post-hoc tests demonstrating *CHRNA5* expression is stronger in chandelier
655 cells compared to all but one other cell type. Mean expression of *CHRNA5* in chandelier cells displayed
656 (red line). ***B,*** Expression of *CHRNA4* (left) and *CHRNB2* (right) across different cell types in the ROS/MAP
657 DLPFC snRNAseq dataset. Mean expression of *CHRNA4* or *CHRNB2* in chandelier cells displayed (red line)**.**
658 Data shown as mean + SEM of the data averaged per cell-type per individual. ***C,*** Expression of *CHRNA5*
659 across cell types in the PFC in individuals split by genotype for the rs1979905 A allele, expression
660 averaged per cell type per individual. Number of individuals per rs1979905 A allele genotype: 0, n = 5; 1,
661 n = 13; 2, n = 4. ***D,*** Effect of genotype for rs1979905 A allele on expression of *CHRNA5* in selected cell
662 types, data shown as *CHRNA5* expression averaged per cell type per individual. A pattern of increasing
663 *CHRNA5* expression with increasing rs1979905 A zygosity is present in some cell types. Significance
664 shown for linear regression models for L5 and L6 excitatory neurons. Displayed as mean + SEM. Number
665 of cells per subtype indicated (n_{cell}).

666 **Figure 3. Chandelier cells are significantly enriched for genes interacting with amyloid. *A,*** Ontology
667 (molecular function) of gene set upregulated in cortical PVALB+ chandelier cells vs. PVALB+ non-
668 chandelier cells. Only molecular functions with significant fold enrichment after FDR are displayed.
669 "Calcium ion-binding" and "amyloid-beta binding" functions are highlighted. ***B,*** Venn diagram displaying
670 genes from ***A*** with either a "calcium ion-binding" or a "amyloid-beta binding" molecular function, and
671 their overlap.

672 **Figure 4. Association of chandelier cell proportions with β-amyloid load is dependent on the**
673 **rs16969968 A allele genotype**. ***A,*** Stratifying by rs16969968 A allele reveals a significant interaction
674 effect between rs16969968 A allele and amyloid load on chandelier cell proportions with rs16969968 A
675 allele homozygotes showing a significantly stronger association between brain amyloid load and

676 chandelier cell proportions compared to rs16969968 A allele non-carriers (t = -2.799, p = 0.005). Scatter
677 plots show 95% confidence intervals of linear model predictions, β-coefficients and p values of individual
678 linear regression models are displayed. ***B*,** Overlay of the linear models from A, showing 95% confidence
679 intervals. ***C*,** Stratifying by rs1979905 A allele reveals a near significant interaction effect between
680 rs1979905 A allele and amyloid load on chandelier cell proportions with rs1979905 A allele homozygotes
681 showing a less negative association between brain amyloid load and chandelier cell proportions
682 compared to rs1979905 A allele non-carriers (t = 1.769, p = 0.078). Scatter plots show 95% confidence
683 intervals of linear model predictions, β-coefficients and p values of individual linear regression models
684 are displayed. ***D***, Overlay of the linear models from C, showing 95% confidence intervals.

685 **Figure 5. A working model of the potential role of chandelier cells in β-amyloid processing, and of the**
686 **impact of *CHRNA5* genotype on chandelier cell (ChC) resilience and vulnerability.** Top: Chandelier cells
687 are significantly enriched for multiple genes involved in β-amyloid processing and degradation including
688 for example neprilysin (NEP), a potentially *CHRNA5*-regulated degrader of β-amyloid, and SORL1, a vital
689 component of the APP-recycling pathway. Bottom: In coding-SNP rs16969968 non-carriers, the α4β2α5
690 nicotinic receptor is resistant to inhibition by β-amyloid, preserving nicotinic signalling even at high β-
691 amyloid levels that inhibit the α4β2 receptors. In coding-SNP rs16969968 homozygous individuals, the
692 disruption of the α5 subunit may reduce its representation in the receptors or block its protective
693 function against β-amyloid, leading to disrupted nicotinic signalling at higher β-amyloid levels, possibly

Table 1. Expression correlation of selected cholinergic genes.

Results of Pearson's correlation analysis of the expression of selected cholinergic genes using the bulk tissue RNAseq data from the DLPFC of ROS/MAP individuals.

Gene 1	Gene 2	r	p	FDR
CHRNA4	*ACHE*	0.556	<0.001	<0.001
	CHRM1	0.542	<0.001	<0.001
	CHRM3	0.242	<0.001	0.002
	CHRNA2	0.307	<0.001	<0.001
	CHRNA7	0.131	0.039	0.464
	CHRNB2	0.457	<0.001	<0.001
CHRNA5	*ACHE*	0.063	0.324	1.000
	CHRM1	-0.309	<0.001	<0.001
	CHRM3	-0.095	0.134	1.000
	CHRNA2	-0.045	0.477	1.000
	CHRNA4	-0.130	0.041	0.464
	CHRNA7	-0.061	0.342	1.000
	CHRNB2	-0.248	<0.001	0.001
CHRNB2	*ACHE*	0.472	<0.001	<0.001
	CHRM1	0.846	<0.001	<0.001
	CHRM3	0.645	<0.001	<0.001
	CHRNA2	0.283	<0.001	<0.001
	CHRNA4	0.457	<0.001	<0.001
	CHRNA7	0.359	<0.001	<0.001

A

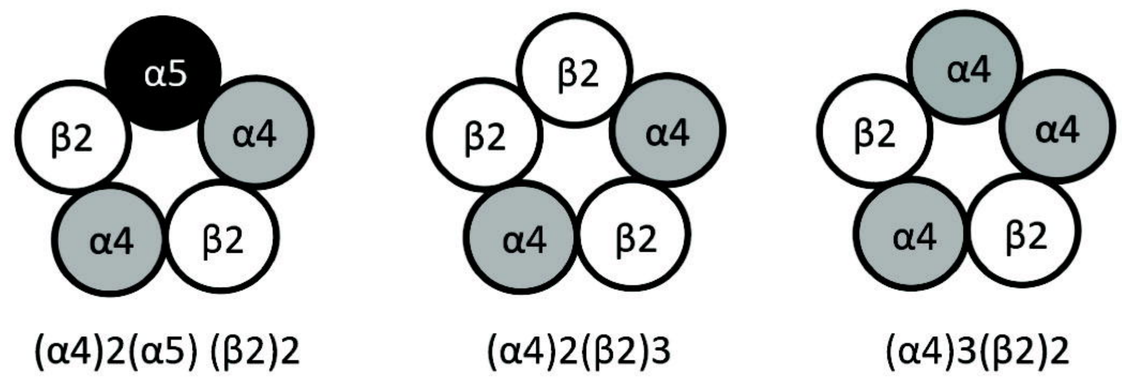

B

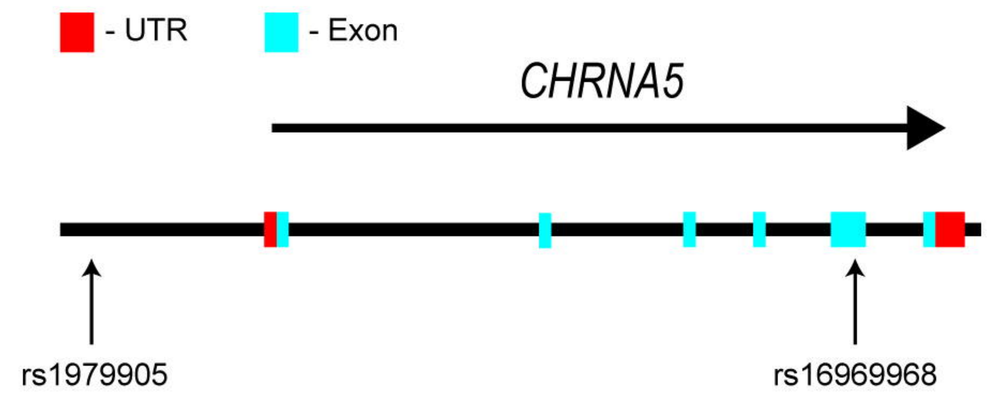

C

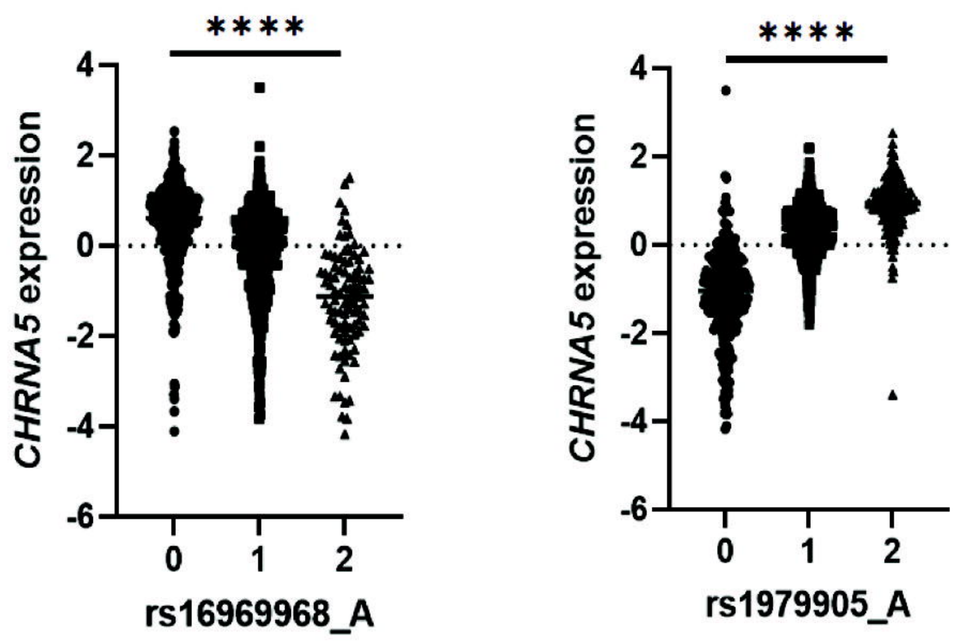

D

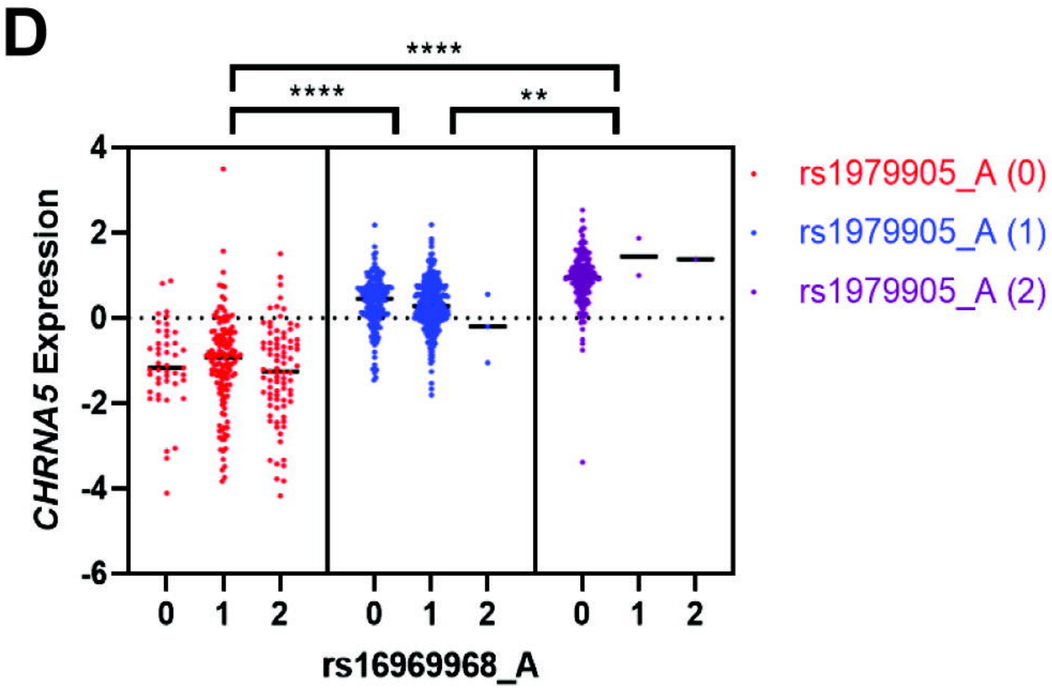

E

SNP/Gene	*CHRNA5*	*CHRNA4*	*CHRNB2*
rs1979905_A	1.083 ($5.94*10^{-124}$)	-	-
rs16969968_A	-0.713 ($3.98*10^{-40}$)	-	-
rs1044396_G	-	0.075 (0.0003)	-
rs4549700_T	-	-0.181 ($1.32 * 10^{-11}$)	-
rs4292956_T	-	-	-0.209 ($2.02*10^{-7}$)
rs2072660_T	-	-	-0.128 ($7.05*10^{-7}$)

F

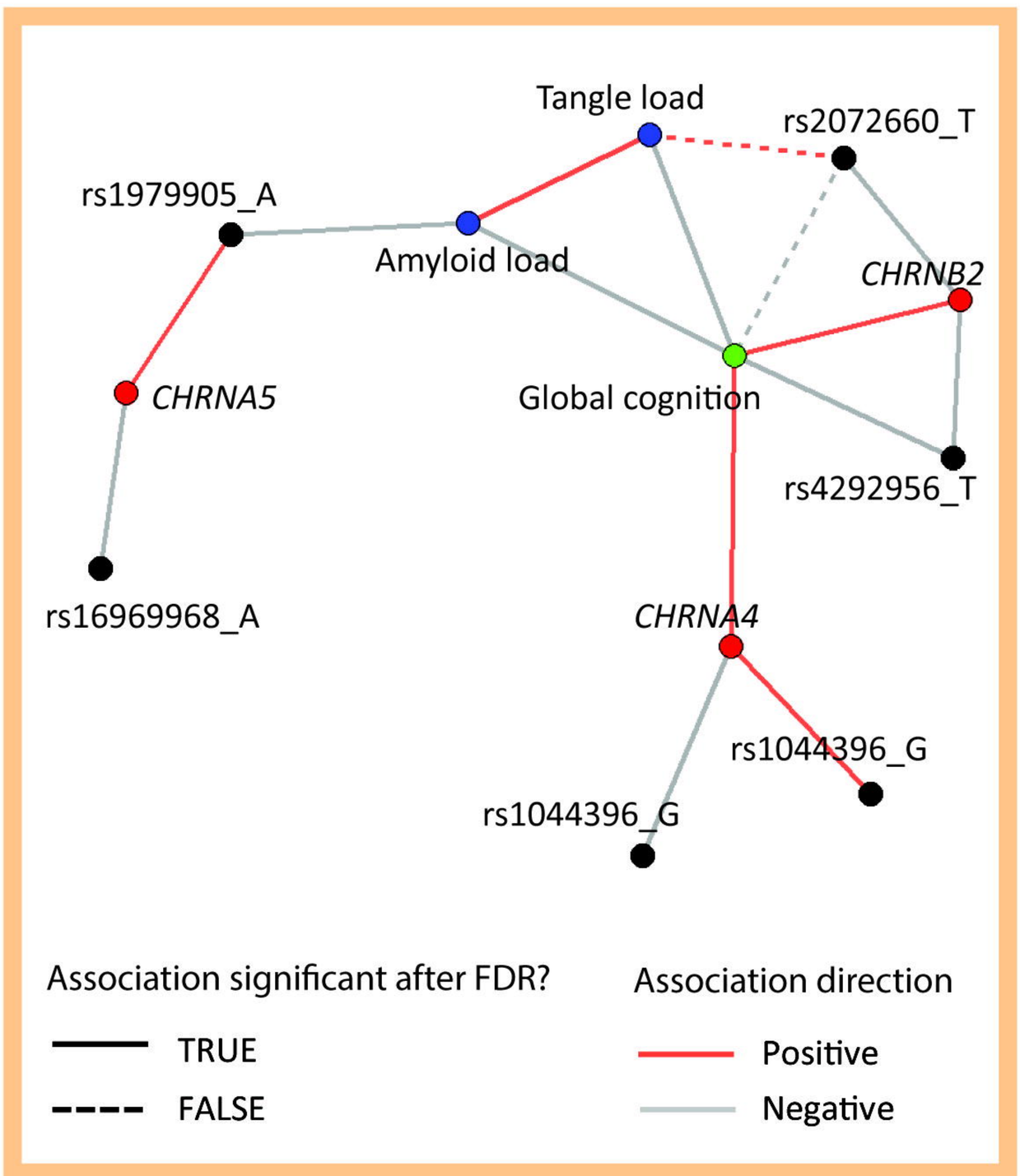

G

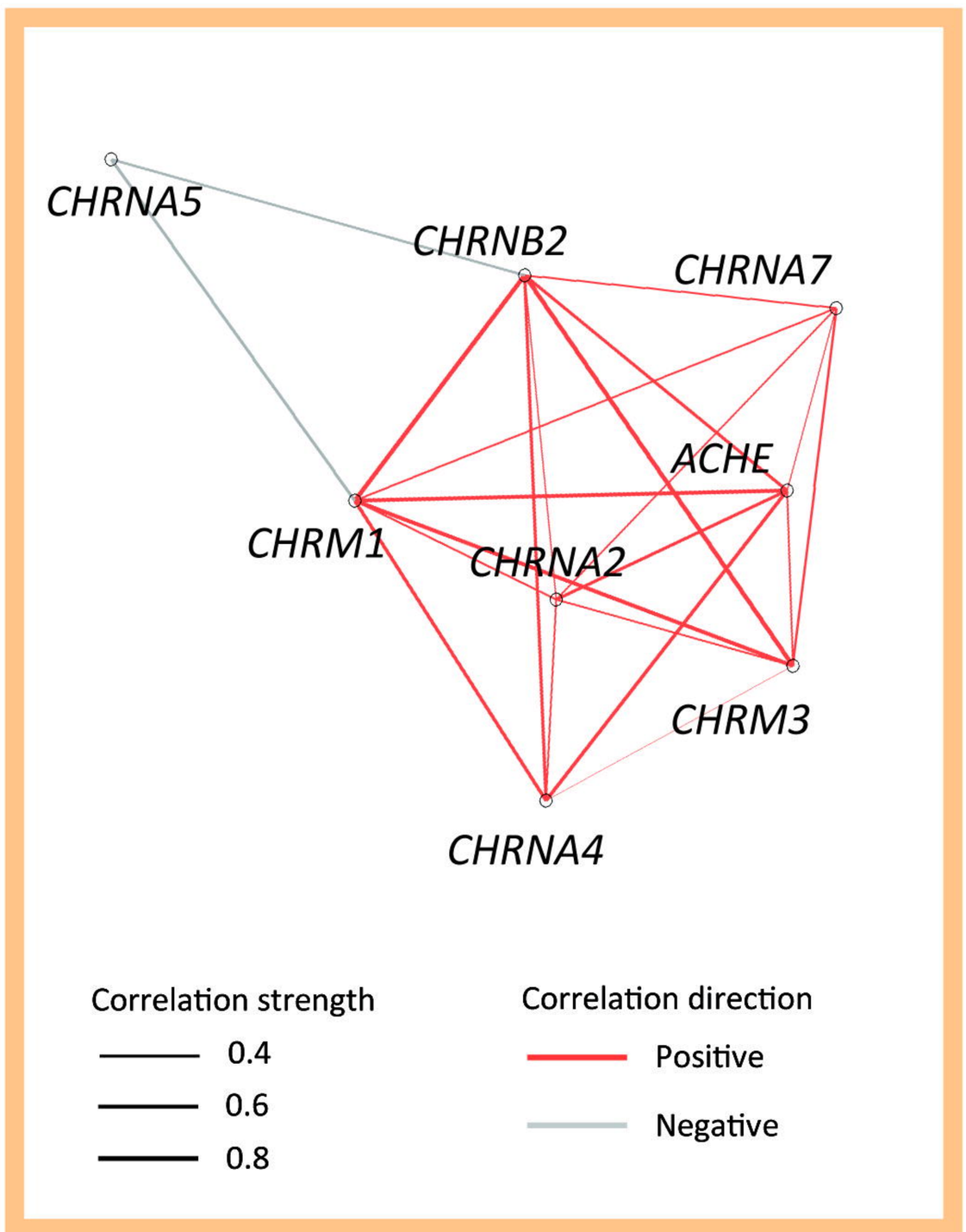

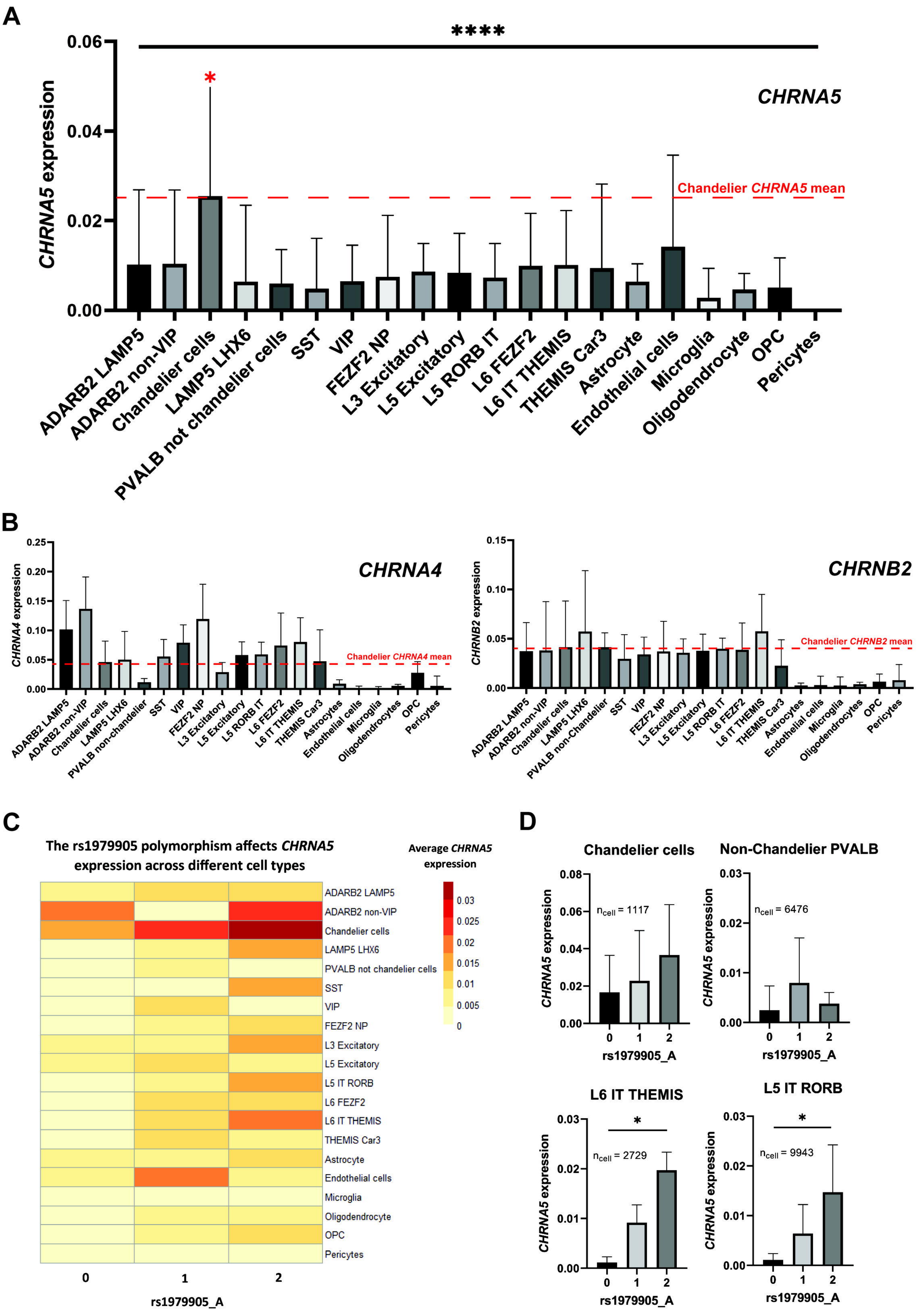
A
****
*
CHRNA5
Chandelier CHRNA5 mean
CHRNA5 expression
0.06
0.04
0.02
0.00
ADARB2 LAMP5
ADARB2 non-VIP
Chandelier cells
LAMP5 LHX6
PVALB not chandelier cells
SST
VIP
FEZF2 NP
L3 Excitatory
L5 Excitatory
L5 RORB IT
L6 FEZF2
L6 IT THEMIS
THEMIS Car3
Astrocyte
Endothelial cells
Microglia
Oligodendrocyte
OPC
Pericytes
B
CHRNA4
Chandelier CHRNA4 mean
CHRNA4 expression
0.25
0.20
0.15
0.10
0.05
0.00
ADARB2 LAMP5
ADARB2 non-VIP
Chandelier cells
LAMP5 LHX6
PVALB non-chandelier
SST
VIP
FEZF2 NP
L3 Excitatory
L5 Excitatory
L5 RORB IT
L6 FEZF2
L6 IT THEMIS
THEMIS Car3
Astrocytes
Endothelial cells
Microglia
Oligodendrocytes
OPC
Pericytes
CHRNB2
Chandelier CHRNB2 mean
CHRNB2 expression
0.15
0.10
0.05
0.00
ADARB2 LAMP5
ADARB2 non-VIP
Chandelier cells
LAMP5 LHX6
PVALB non-Chandelier
SST
VIP
FEZF2 NP
L3 Excitatory
L5 Excitatory
L5 RORB IT
L6 FEZF2
L6 IT THEMIS
THEMIS Car3
Astrocytes
Endothelial cells
Microglia
Oligodendrocytes
OPC
Pericytes
C
The rs1979905 polymorphism affects CHRNA5 expression across different cell types
Average CHRNA5 expression
0.03
0.025
0.02
0.015
0.01
0.005
0
ADARB2 LAMP5
ADARB2 non-VIP
Chandelier cells
LAMP5 LHX6
PVALB not chandelier cells
SST
VIP
FEZF2 NP
L3 Excitatory
L5 Excitatory
L5 IT RORB
L6 FEZF2
L6 IT THEMIS
THEMIS Car3
Astrocyte
Endothelial cells
Microglia
Oligodendrocyte
OPC
Pericytes
0
1
2
rs1979905_A
D
Chandelier cells
CHRNA5 expression
n_{cell} = 1117
0.08
0.06
0.04
0.02
0.00
0
1
2
rs1979905_A
Non-Chandelier PVALB
CHRNA5 expression
n_{cell} = 6476
0.03
0.02
0.01
0.00
0
1
2
rs1979905_A
L6 IT THEMIS
CHRNA5 expression
*
n_{cell} = 2729
0.03
0.02
0.01
0.00
0
1
2
rs1979905_A
L5 IT RORB
CHRNA5 expression
*
n_{cell} = 9943
0.03
0.02
0.01
0.00
0
1
2
rs1979905_A

A

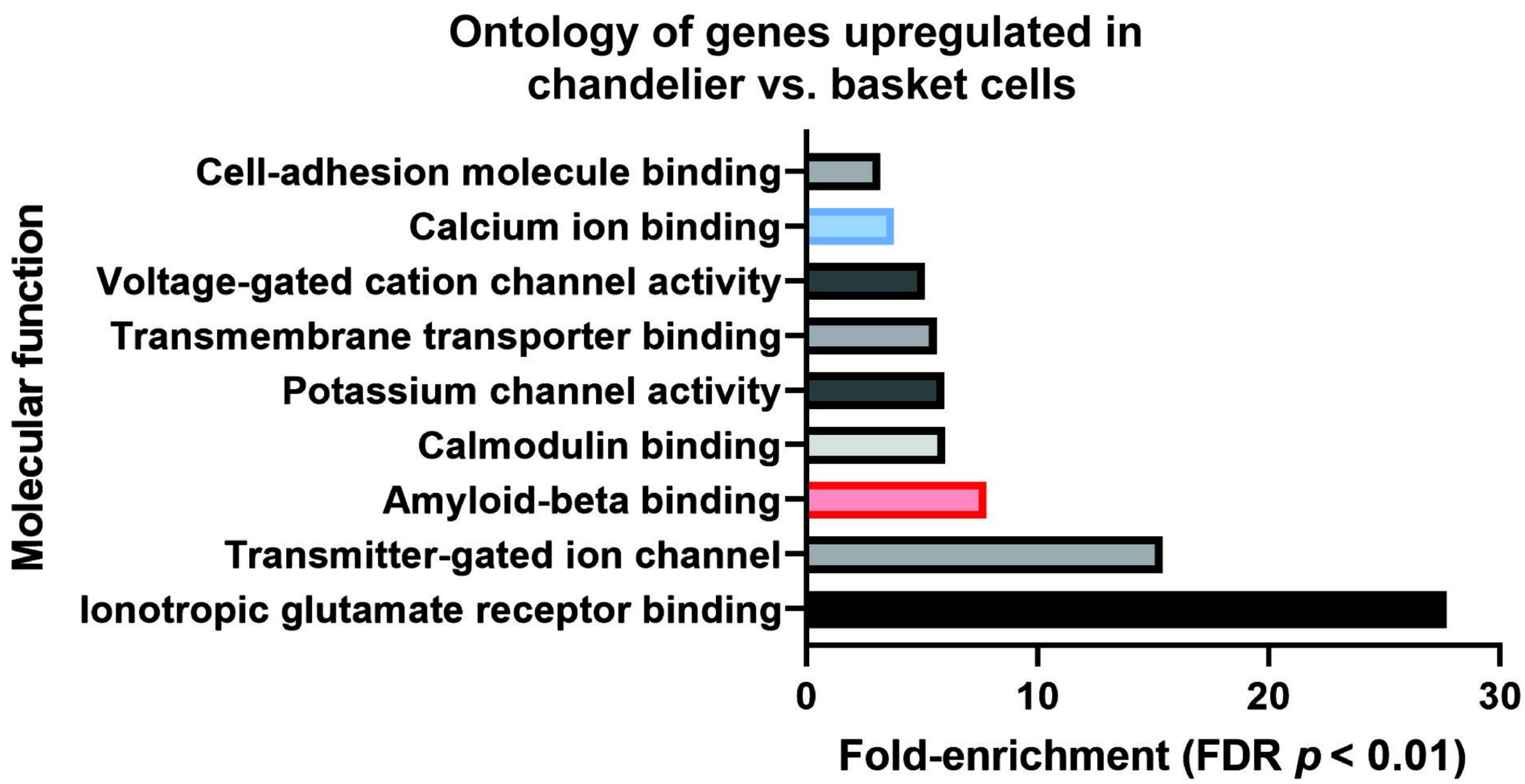
Ontology of genes upregulated in chandelier vs. basket cells
Molecular function
Cell-adhesion molecule binding
Calcium ion binding
Voltage-gated cation channel activity
Transmembrane transporter binding
Potassium channel activity
Calmodulin binding
Amyloid-beta binding
Transmitter-gated ion channel
Ionotropic glutamate receptor binding
0
10
20
30
Fold-enrichment (FDR p < 0.01)

B

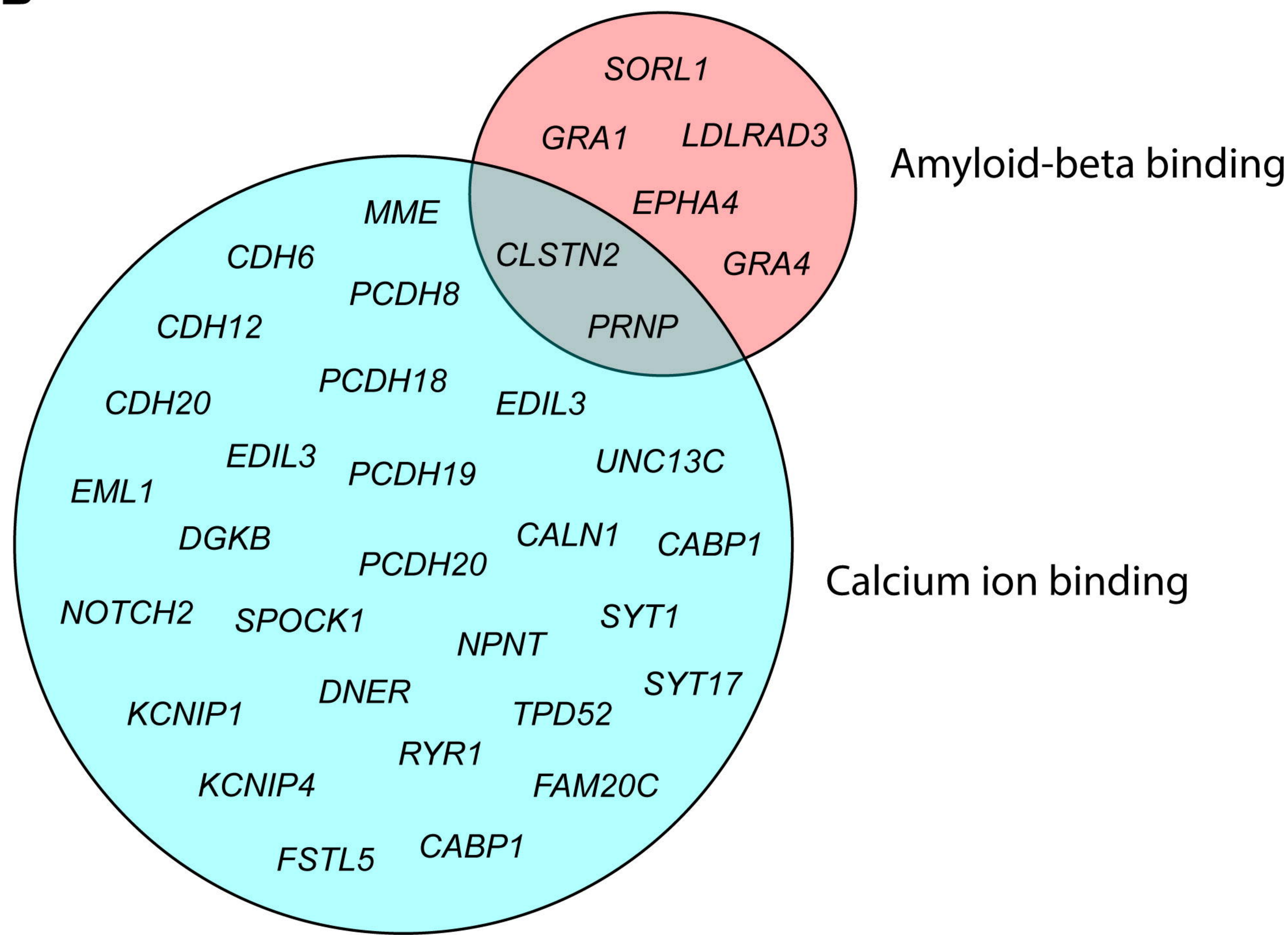
SORL1
GRA1
LDLRAD3
EPHA4
GRA4
Amyloid-beta binding
MME
CDH6
CLSTN2
PCDH8
CDH12
PRNP
PCDH18
CDH20
EDIL3
EDIL3
PCDH19
UNC13C
EML1
DGKB
CALN1
CABP1
PCDH20
NOTCH2
SPOCK1
SYT1
NPNT
DNER
SYT17
KCNIP1
TPD52
RYR1
KCNIP4
FAM20C
FSTL5
CABP1
Calcium ion binding

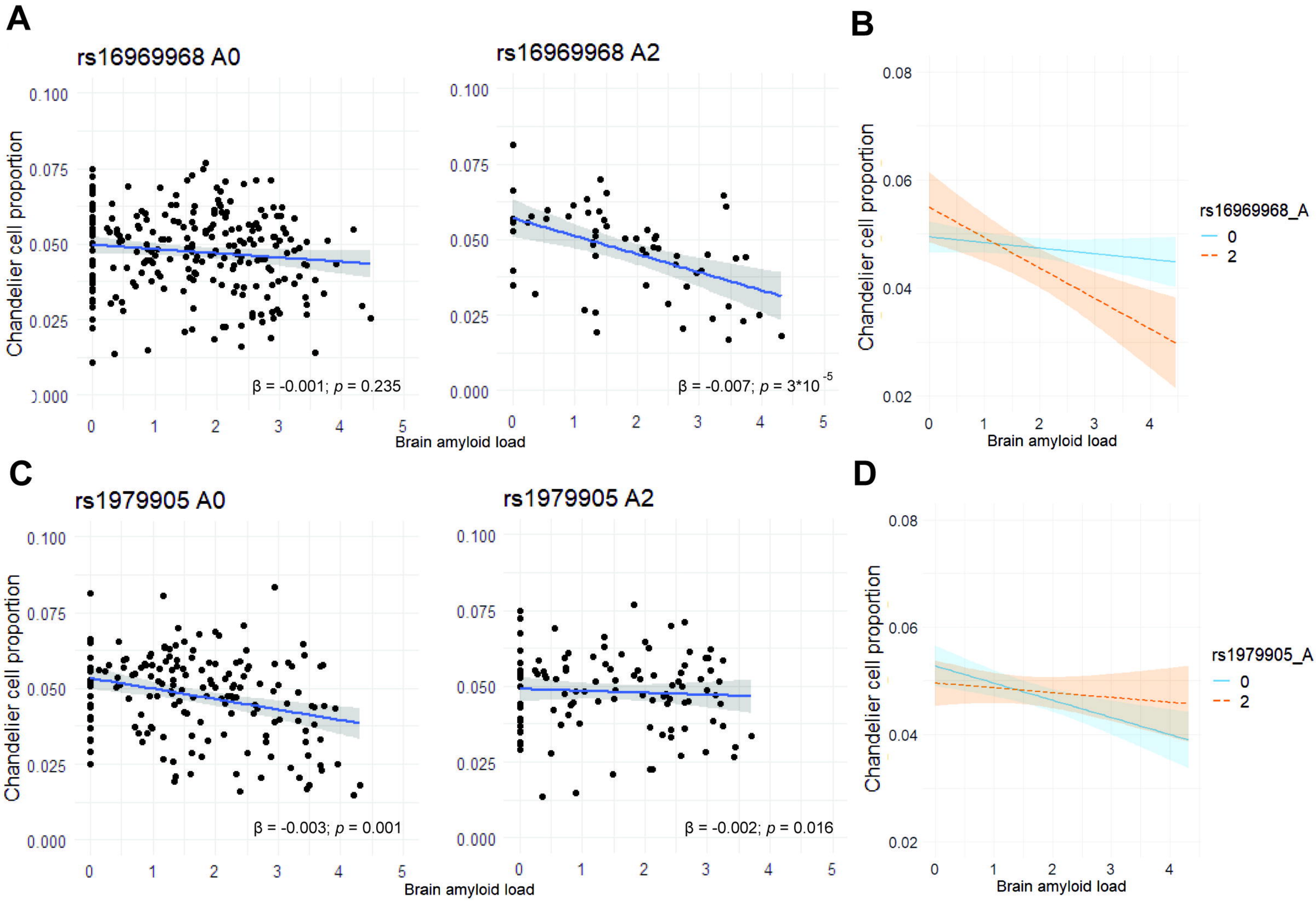
A
rs16969968 A0
rs16969968 A2
Chandelier cell proportion
Brain amyloid load
β = -0.001; p = 0.235
β = -0.007; p = 3*10^-5
B
rs16969968_A
0
2
C
rs1979905 A0
rs1979905 A2
β = -0.003; p = 0.001
β = -0.002; p = 0.016
D
rs1979905_A
0
2

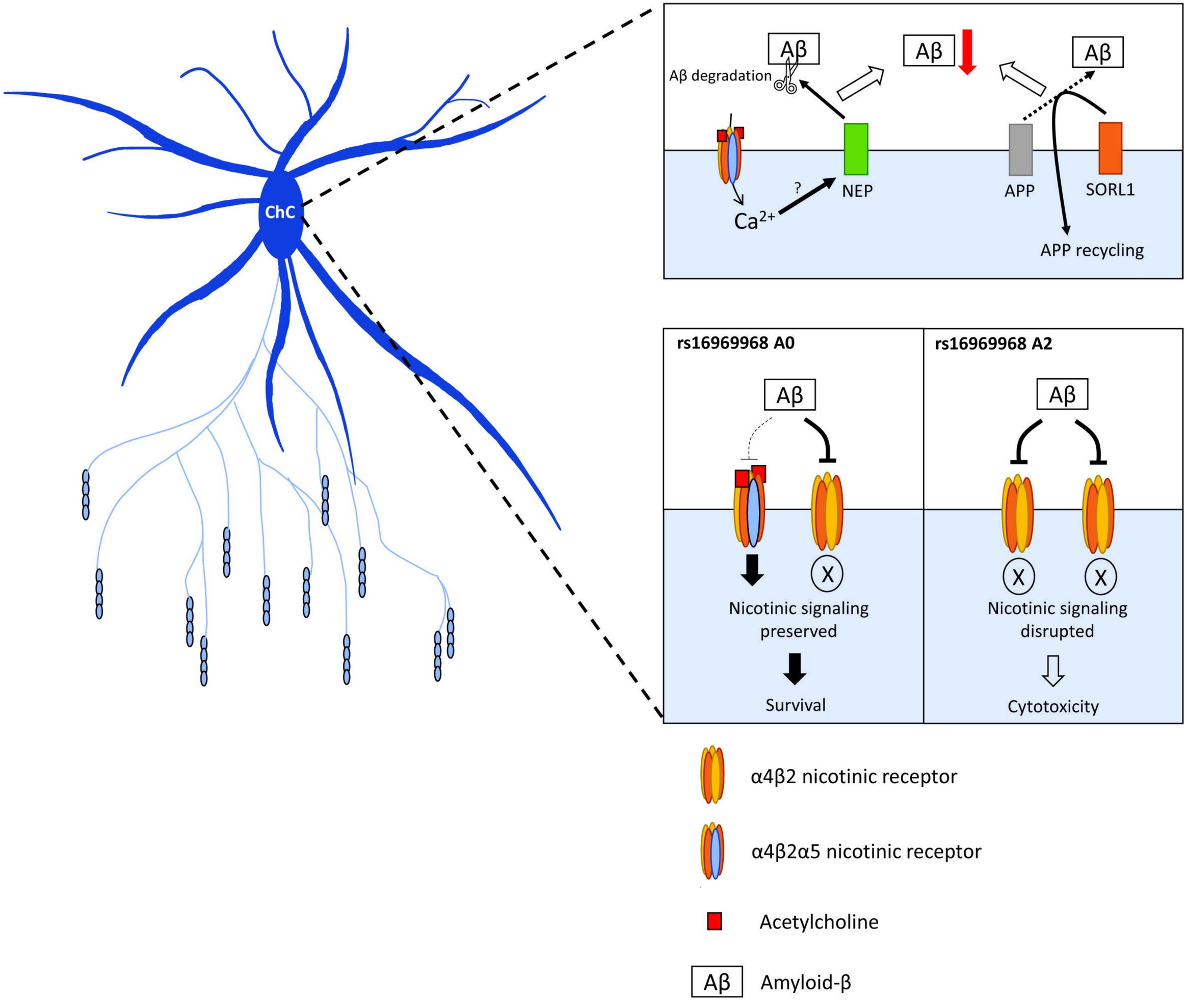
ChC
Aβ
Aβ degradation
Aβ
Aβ
Ca2+
?
NEP
APP
SORL1
APP recycling
rs16969968 A0
rs16969968 A2
Aβ
Aβ
X
X
X
Nicotinic signaling preserved
Nicotinic signaling disrupted
Survival
Cytotoxicity
α4β2 nicotinic receptor
α4β2α5 nicotinic receptor
Acetylcholine
Aβ
Amyloid-β